

The Structures of Difluorodiisocyanatomethane, $\text{CF}_2(\text{NCO})_2$: X-ray Crystallography, Gas Electron Diffraction, and Quantum Chemical Calculations

Jürgen Buschmann,[†] Dieter Lentz,[‡] Peter Luger,[†] Matthias Röttger,[‡] and Heinz Oberhammer^{*,†,¶}

Fachbereich Biologie, Chemie, Pharmazie, Institut für Chemie—Anorganische und Analytische Chemie, Freie Universität Berlin, Fabeckstrasse 34–36, D-14195 Berlin, Germany, Fachbereich Biologie, Chemie, Pharmazie, Institut für Chemie—Kristallographie, Freie Universität Berlin, Takustrasse 6, D-14195 Berlin, Germany, and Institut für Physikalische und Theoretische Chemie, Universität Tübingen, Auf der Morgenstelle 8, D-72076 Tübingen, Germany

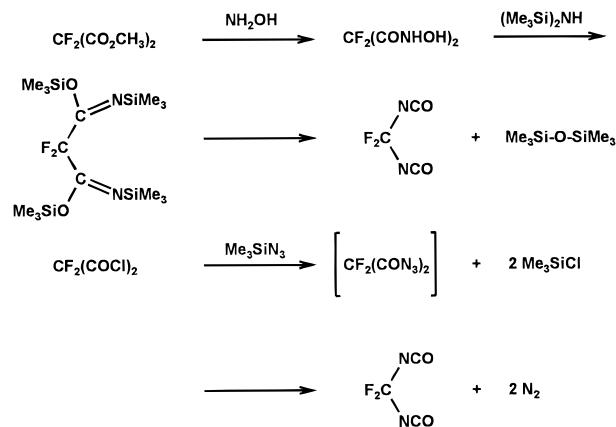
Received: February 23, 2000; In Final Form: May 9, 2000

Difluorodiisocyanatomethane was prepared by reaction of difluoromalonyl chloride with trimethylsilyl azide. Its molecular structure was determined by X-ray crystallography at 141 K and by gas electron diffraction (GED), and quantum chemical calculations were performed at different levels of theory. Difluorodiisocyanatomethane crystallizes monoclinic, space group $P2_1$, $a = 7.900(4)$, $b = 4.890(3)$, $c = 12.601(7)$ Å, $\beta = 102.280(10)^\circ$, $V = 475.7(5)$ Å³, $R_1 = 0.0429$, $wR_2 = 0.1179$. The asymmetric unit consists of two molecules with C_1 symmetry that are enantiomers. They differ only by the sign of related dihedral N–C–N=C angles, which describe the orientations of the two N=C=O groups: $\Phi_1 = 107.2(2)^\circ$, $\Phi_2 = -4.8(2)^\circ$ for molecule A and $\Phi_1 = -103.9(2)^\circ$, $\Phi_2 = 8.9(2)^\circ$ for molecule B. The GED analysis results in a mixture of two conformers, 72(12)% possessing C_1 symmetry ($\Phi_1 = 131(4)^\circ$, $\Phi_2 = 43(5)^\circ$) and 28(12)% possessing C_2 symmetry ($\Phi_1 = \Phi_2 = 52(8)^\circ$). Bond lengths and bond angles in the solid state and in the gas phase are very similar, but dihedral angles differ by almost 50° . Quantum chemical calculations (HF, MP2, B3PW91, and B3LYP with different basis sets) reproduce the conformational composition, bond lengths, and bond angles very well. Predicted dihedral angles, however, depend strongly on the computational method and none of the calculations reproduces the experimental gas-phase values satisfactorily. They demonstrate, nevertheless, that the potential surface for internal rotation around the two C–N bonds is very flat.

Introduction

Isocyanates are important industrial chemicals for the synthesis of polyurethanes prepared in large scale by phosgenation of amines.¹ Laboratory methods for their synthesis are often based on the Curtius, Hofmann or Lossen Rearrangement.² There exist a few geminal diisocyanates, such as diisocyanatomethane³ or 1,2,2 trisocyanatobutane,⁴ prepared by a Curtius Rearrangement as geminal diamines that are highly unstable. Because α -fluoroamines such as trifluoromethylamine⁵ are unstable, the preparation of α -fluorinated isocyanates such as trifluoromethyl isocyanate⁶ is based on the Curtius Rearrangement. This preparation, however, needs acyl azide precursors that are reported to be capriciously explosive.⁷ Middleton et al. reported a general synthesis of perfluorinated isocyanates, including the title compound, by pyrolysis of disilyl esters of hydroxamic acids,⁸ a modification of the Lossen Rearrangement.⁹ So far, only two structural studies of geminal diisocyanates of the group 14 elements have been reported, one for $\text{Cl}_2\text{Si}(\text{NCO})_2$ ¹⁰ in the gas phase and one for $[(\text{Me}_3\text{Si})_2\text{CH}]_2\text{Sn}(\text{NCO})_2$ ¹¹ in the solid state. In the present study we report on the geometric structure and conformational properties of difluorodiisocyanatomethane that were studied experimentally in the solid state by X-ray diffraction and in the gas phase by gas

SCHEME 1



electron diffraction (GED). Furthermore, quantum chemical calculations with different computational methods and different basis sets were performed.

Syntheses

The syntheses of $\text{CF}_2(\text{NCO})_2$ are outlined in Scheme 1. The procedure described by Middleton is based on a 0.5 to 1 mol scale. After many unsuccessful attempts to prepare difluorodiisocyanatomethane by the method of Middleton on a millimole scale we decided to use the Curtius Rearrangement for the synthesis of $\text{CF}_2(\text{NCO})_2$ using the stable trimethylsilyl azide as

* Corresponding author. FAX +49 7071 295490; E-mail: heinz.oberhammer@uni-tuebingen.de.

[†] Kristallographie, Berlin.

[‡] Anorganische und Analytische Chemie, Berlin.

[¶] Tübingen.

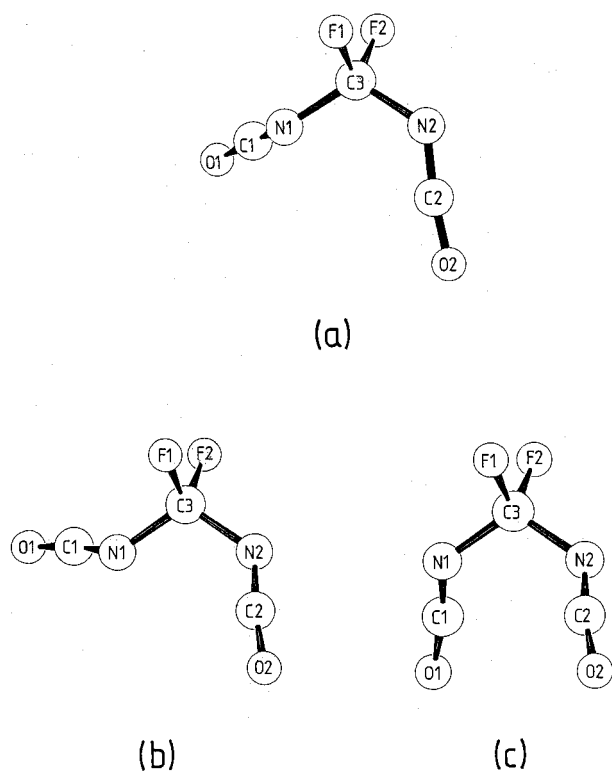


Figure 1. Molecular structure of difluorodiisocyanatomethane; (a) solid state, molecule A; (b) gas-phase C_1 symmetrical conformer; (c) gas-phase C_2 symmetrical conformer.

the N_3 transferring agent without isolating the explosive acyl azide. In that way millimole quantities of $CF_2(NCO)_2$ can be synthesized. However, the $CF_2(NCO)_2$ is contaminated with trimethylsilyl chloride and trimethylsilyl fluoride. To obtain an analytically pure sample, further purification using a preparative gas-liquid chromatography (GLC) is essential.

Quantum Chemical Calculations

Geometry optimizations were performed with the Hartree-Fock (HF) and Moller-Plesset (MP2) approximations and density functional hybrid methods B3PW91 and B3LYP with 6-31G* basis sets, using the Gaussian 98 program suite.¹² Various starting values for the dihedral angles $\Phi_1(N2-C3-N1=C1)$ and $\Phi_2(N1-C3-N2=C2)$ were chosen as input to cover the entire conformational space (see Figure 1 for atom numbering). All methods predict two stable conformations. According to the HF approximation, these structures possess C_2 symmetry with $\Phi_1 = \Phi_2$ and C_s symmetry, with $\Phi_1 = 0^\circ$ and $\Phi_2 = 180^\circ$. Inclusion of electron correlation in the MP2 approximation or with density functional (DFT) methods leads to two conformers with C_2 and C_1 symmetry. The calculated energy differences between the two structures are very small, (<0.15 kcal mol⁻¹). In a later stage of this study, additional MP2 and B3LYP calculations with larger basis sets were performed. Bond lengths and bond angles of the main conformer (C_1 symmetry) obtained with the MP2 and B3LYP methods and 6-311G(2df) basis sets and the dihedral angles for both conformers and their relative energies predicted by the different computational methods are listed together with the corresponding experimental values (vide infra). Vibrational frequencies were calculated with the B3PW91 approximation. The Cartesian force constants were transformed to symmetry force constants, and vibrational amplitudes were derived with the program ASYM40.¹³ Thereby, the dihedral angles obtained from the GED experiment were used for the

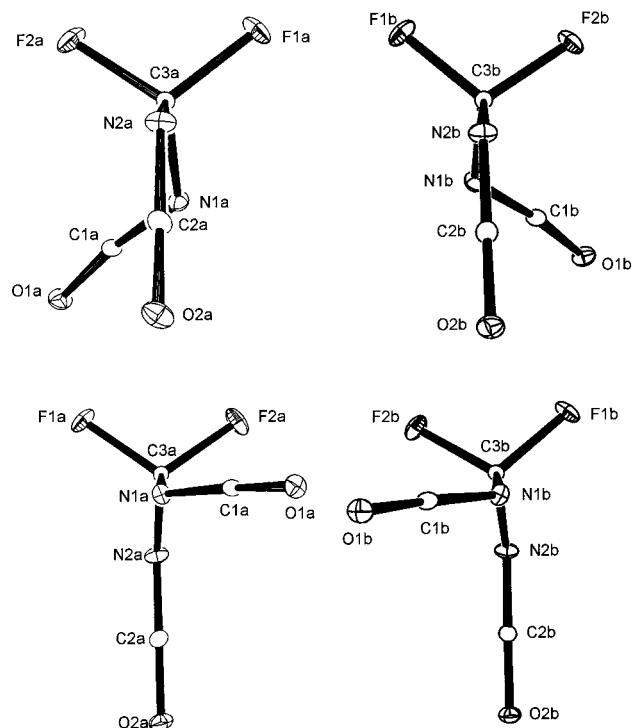


Figure 2. ORTEP illustration (10% ellipsoids chosen for clarity) of the two enantiomeric molecules A and B of $CF_2(NCO)_2$ present in the unit cell. View approximately along the N-C3 bonds to show the important torsional angles.

two conformers. The amplitudes for the C_1 conformer are included as Supporting Information.

Crystal Structure

Difluorodiisocyanatomethane is a colorless liquid at ambient temperature. A crystal suitable for X-ray crystallography was obtained by slow crystallization of the liquid in a glass capillary [inner diameter (i.d.), 0.3 mm] in a temperature gradient close to the melting point of 150 K. Difluorodiisocyanatomethane crystallizes monoclinic, space group $P2_1$, with two molecules in the asymmetric unit.

A total of 7274 reflections of little more than a half sphere were collected up to $\theta = 45.52^\circ$ and merged to 4292 unique reflections ($R_{int} = 0.0213$). The structure was solved by direct methods (SHELXS 97¹⁴) and refined on F^2 by full-matrix least-squares methods (SHELXL 97¹⁵) using anisotropic displacement parameters for all atoms. The refinement converged at $wR_2 = 0.1179$ for 163 parameters and 4292 unique reflections, and $R_1 = 0.0429$ for 2721 observed reflections with $F_o^2 > 2\sigma(F_o^2)$. Details of the data collection and refinement are given in Table 1 and as Supporting Information.

The molecular structure of molecule A is shown in Figure 1, compared with results obtained by GED. Figure 2 represents a view of the two molecules almost along the $N1-C3$ and $N2-C3$ bonds, respectively, showing the important torsional angles. The packing diagram is shown in Figure 3. From Figures 2 and 3 it is obvious that the two molecules forming the asymmetric unit differ only by the sign of related torsional angles and thus are enantiomers. Therefore, it is surprising that difluorodiisocyanatomethane crystallizes in the chiral space group $P2_1$. However, on checking for additional crystallographic symmetry elements using the program PLATON,¹⁶ no additional symmetry was found. Related individual bond lengths and angles, except $C-N=C$ and $N=C=O$, are equal within 3σ and thus have been averaged as listed in Table 2 together with the GED and ab

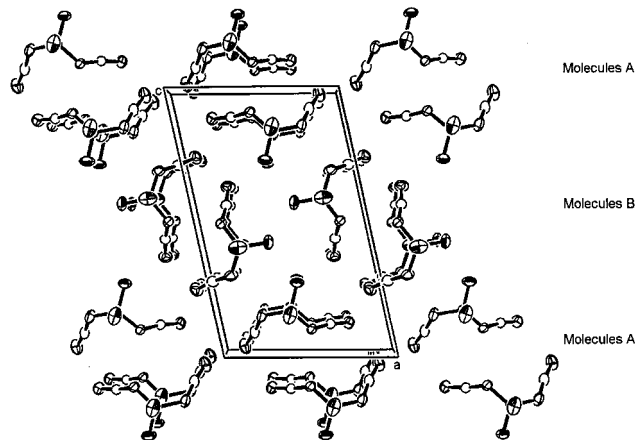
TABLE 1: Crystal Data and Structure Refinement for Difluorodiisocyanatomethane

parameter	value	
empirical formula	C ₃ F ₂ N ₂ O ₂	
formula weight	134.05	
temperature	141(1) K	
wavelength	0.71069 Å	
crystal system	monoclinic, second setting	
space group	P2 ₁	
unit cell dimensions	$a = 7.900(4)$ Å	$\alpha = 90^\circ$
	$b = 4.890(3)$ Å	$\beta = 102.280(10)^\circ$
	$c = 12.601(7)$ Å	$\gamma = 90^\circ$
volume	475.7(5) Å ³	
Z	4	
density (calculated)	1.872 Mg/m ³	
absorption coefficient	0.203 mm ⁻¹	
F(000)	264	
crystal size	endless column $d = 0.3$ mm, $l = 3$ mm	
theta range for data collection	2.64 to 45.52°	
index ranges	$-15 \leq h \leq 13$, $-1 \leq k \leq 9$, $-25 \leq l \leq 25$	
reflections collected	7269	
independent reflections	4292 [$R(\text{int}) = 0.0213$]	
completeness to theta = 45.52°	96.5%	
absorption correction	not done	
refinement method	full-matrix least-squares on F^2	
data/restraints/parameters	4292/1/163	
goodness-of-fit on F^2	0.970	
final R indices [$I > 2\sigma(I)$]	$R_1 = 0.0429$, $wR_2 = 0.1058$	
R indices (all data)	$R_1 = 0.0726$, $wR_2 = 0.1179$	
absolute structure parameter	-0.2(5)	
extinction coefficient	none	
largest diff. peak and hole	0.486 and -0.230 eÅ ⁻³	

TABLE 2: Experimental and Calculated Bond Lengths and Bond Angles for the C₁ Conformer of CF₂(NCO)₂ (mean values; dihedral angles are given in Table 3)

parameter	X-ray ^a	GED ^b	MP2/	B3LYP/
			6-311G(2df)	6-311G(2df)
C–F	1.345(2)	1.354(2)	1.343	1.354
C–N	1.410(2)	1.407(3)	1.410	1.415
N=C	1.210(2)	1.207(2)	1.219	1.213
C=O	1.155(2)	1.168(3)	1.162	1.157
N–C3–N	114.9(1)	111.6(13)	111.8	112.7
F–C–F	105.7(1)	106.4 ^c	106.4	106.0
C3–N1=C1	130.0(1)	127.7(12) ^d	127.9	131.1
C3–N2=C2	127.9(1)	127.1(12) ^d	127.3	129.7
N1=C1=O1	172.2(2)	171.7(26) ^e	173.0	173.4
N2=C2=O2	173.5(2)	171.7(26) ^e	173.2	173.7

^a r_σ parameters in Å and degree with σ values. ^b r_σ parameters with 3σ values. ^c Assumed. ^d Difference (C3–N1=C1) – (C3–N2=C2) constrained to 0.6° (MP2 value). ^e Assumed to be equal.

Figure 3. Unit cell of CF₂(NCO)₂ (ORTEP, 50% ellipsoids). View along 010.

into data for comparison. Torsional angles of the individual molecules A and B are given in Table 3. The fractional

TABLE 3: Experimental and Calculated Dihedral Angles Φ_1 (N–C3–N1=C1) and Φ_2 (N1–C3–N2=C2) and Relative Stability of C₂ and C₁ Conformers

method	C ₁ conformer		C ₂ conformer	$\Delta H^\circ/\Delta E$ (kcal mol ⁻¹) ^a
	Φ_1	Φ_2	$\Phi_1 = \Phi_2$	
crystal, molecule A	107.2(2)	-4.8(2)	—	—
crystal, molecule B	-103.9(2)	8.9(2)	—	—
gas phase	131(4)	43(5)	52(8)	0.15(18)
HF/6-31G*	180	0	93	-0.03
MP2/6-31G*	164	61	83	+0.02
MP2/6-311G(2df)	173	42	68	-0.13
B3PW91/6-31G*	161	44	84	-0.10
B3LYP/6-31G*	125	64	89	+0.06
B3LYP/6-311G(2df)	172	19	79	+0.05

$$^a \Delta H^\circ = H^\circ(C_2) - H^\circ(C_1).$$

coordinates and equivalent thermal parameters are listed in Table 4. A full list of all geometrical parameters and thermal displacement factors can be found in the Supporting Information.

The F1–C3 vector (Figure 3) of both molecules in the asymmetric unit is oriented almost parallel to the b axis of the monoclinic unit cell. Looking along the F1–C3 bond the NCO groups form left- and right-handed screws for the molecules A and B, respectively. Molecules of type A related by the 2-fold screw axis, and translations along a and b form a double layer between $-0.25 < z < 0.25$ separated by a layer of molecules B between $0.25 < z < 0.75$. There exist no unusual short intermolecular contacts between the individual molecules.

Gas-Phase Structure

The radial distribution function (RDF) was derived by Fourier transformation of the molecular intensities. Comparison with calculated curves for the C₁ and C₂ conformer (Figure 4) shows that the C₁ conformer is the main component. The peak at ~2.9 Å and the shoulder at about 3.9 Å in the experimental RDF indicate a substantial contribution from the C₂ form with a

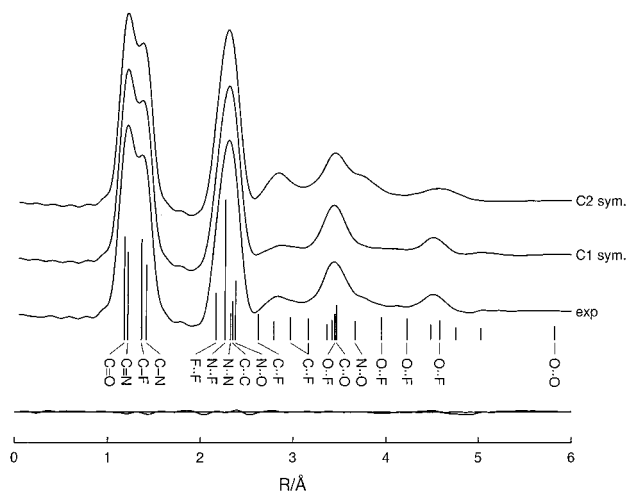


Figure 4. Calculated and experimental radial distribution function and difference curve for mixture of 78% C_1 and 28% C_2 conformer. Important interatomic distances for the C_1 conformer are indicated by vertical bars.

TABLE 4: Atomic Coordinates ($\times 10^4$) and Equivalent Isotropic Displacement Parameters ($\text{\AA}^2 \times 10^3$) for Difluorodicyanatomethane (U_{eq} is defined as one third of the trace of the orthogonalized U^{ij} tensor)

location	<i>x</i>	<i>y</i>	<i>z</i>	U_{eq}
C(1A)	6548(1)	14471(2)	1137(1)	21(1)
C(2A)	1984(1)	14381(3)	849(1)	25(1)
C(3A)	4389(1)	11756(2)	1701(1)	19(1)
F(1A)	4345(1)	9016(2)	1597(1)	39(1)
F(2A)	5129(1)	12249(3)	2743(1)	43(1)
N(1A)	5389(1)	12800(2)	987(1)	24(1)
N(2A)	2664(1)	12694(3)	1504(1)	31(1)
O(1A)	7655(1)	16030(2)	1153(1)	31(1)
O(2A)	1197(1)	15961(2)	265(1)	37(1)
C(1B)	2065(2)	9753(3)	5631(1)	25(1)
C(2B)	346(2)	9622(3)	2840(1)	25(1)
C(3B)	2341(1)	7057(2)	4111(1)	21(1)
F(1B)	2302(2)	4303(2)	4105(1)	40(1)
F(2B)	4027(1)	7744(3)	4272(1)	40(1)
N(1B)	1587(1)	7970(3)	4967(1)	26(1)
N(2B)	1498(2)	7951(3)	3070(1)	31(1)
O(1B)	2357(2)	11398(3)	6305(1)	35(1)
O(2B)	-742(1)	11176(2)	2521(1)	35(1)

dihedral angle $\Phi_1 = \Phi_2$ of $\sim 50^\circ$. Preliminary structural models that are based on analysis of the RDF were then refined by least-squares fitting of the molecular intensities. Different options exist for such a refinement. (1) rigid model without vibrational corrections (r_a structure), (2) rigid model including vibrational corrections (r_α structure), or (3) dynamic model (r_a or r_α structure). The conventional approximation for calculating vibrational corrections, which is based on perpendicular amplitudes, cannot be applied for a compound with two large amplitude motions such as the two torsional vibrations around the C–N bonds. In this case, a curvilinear approach¹⁷ would be appropriate. However, the largest contributions to these corrections come from the two torsional vibrations that have not been observed experimentally. The calculated (B3PW91/6-31G*) torsional frequencies of 22 and 30 cm^{-1} for the C_1 form and of 24 and 28 cm^{-1} for the C_2 structure may be quite inaccurate and thus do not allow the calculation of reliable corrections. The respective lower frequency for the C_1 form is predicted as 15 cm^{-1} by the MP2/6-31G*, compared with 22 cm^{-1} by the B3PW91 method. Obviously, the best option would be a dynamic model. The two large amplitude torsional motions in $\text{CF}_2(\text{NCO})_2$ can be described by a two-dimensional potential function, $V(\Phi_1, \Phi_2)$, in which interaction terms are certainly very

important. In this case, a realistic description of the potential requires seven parameters.¹⁸ Because different quantum chemical methods predict rather different equilibrium structures (vide infra), we cannot expect reliable information about the potential function for internal rotation from these calculations, which could be used as constraints in the GED analysis. On the other hand, it is impossible to derive such a complicated potential function from GED intensities alone. Therefore, we decided to fit the intensities with a rigid model without vibrational corrections (r_a structure). The derived dihedral angles are vibrational averages, and such “effective” values cannot be compared directly with calculated equilibrium values. Experience with other compounds that have been analyzed with rigid and dynamic models shows that effective dihedral angles may deviate from equilibrium values by up to $\sim 20^\circ$.

In the least squares refinement, the geometric parameters of the prevailing C_1 conformer and the dihedral angle $\Phi_1 = \Phi_2$ for the C_2 structure were refined. Mean values for the C–N, C–F, N=C, and C=O bond lengths and for the C–N=C, N–C–F, and N=C=O angles were derived. The differences between the individual parameters (e.g., between C3–N1 and C3–N2) were constrained to the MP2/6-311G(2df) results. Bond lengths and bond angles of the C_2 conformer were tied to the respective values for the C_1 structure using the calculated differences. The F–C–F angle caused high correlations with other parameters and was therefore constrained to the calculated angle. Vibrational amplitudes that caused high correlations between parameters or that were badly determined in the GED experiment and all amplitudes for the C_2 conformer were constrained to calculated values. With these assumptions, 10 geometric parameters and four vibrational amplitudes were refined simultaneously. The following correlation coefficients had absolute values >0.6 : N=C/C=O = -0.61 , NCN/CNC = -0.62 , NCN/NCO = 0.71, and CNC/NCO = -0.76 . Least squares refinements were performed with different but fixed contributions of the C_2 conformer. The lowest *R* factor was obtained for a contribution of 28(12)%. The uncertainty is derived with the Hamilton test at a 1% significance level.¹⁹ The final results for the geometric parameters are listed in Tables 2 and 3. Vibrational amplitudes are available as Supporting Information.

Discussion

The most interesting structural feature of $\text{CF}_2(\text{NCO})_2$ is the orientation of the two NCO groups. The orientation of an NCO group relative to the bonds around the central carbon atom depends primarily on two opposing effects: (1) The general anomeric effect;²⁰ that is, stereoelectronic interaction between the nitrogen lone pair and the antibonding σ^* orbital of an opposite C–F or C–N bond, $[\text{lp}(\text{N}) \rightarrow \sigma^*(\text{C}-\text{X})]$, X = F or N] favors eclipsed orientations with $\Phi(\text{N}-\text{C}-\text{N}=\text{C}) = 0^\circ$ or 120° . In these orientations the lone pair adopts an ideal trans position to one of the C–X bonds. (2) Steric repulsions, however, favor staggered orientations with $\Phi = 180^\circ$ or 60° . CF_3NCO is a molecule in which these two effects nearly compensate each other, resulting in almost free internal rotation around the C–N bond, with a barrier of only 0.14 kcal mol^{-1} .²¹ In $\text{CF}_2(\text{NCO})_2$, additional interactions between the two NCO groups have to be considered. These interactions make doubly eclipsed structures with $\Phi_1 = \Phi_2 = 0^\circ$ and structures with both NCO groups in staggered orientation and $\Phi_1 = \Phi_2 = 180^\circ$ unfavorable because of repulsion between the two NCO groups or between the two nitrogen lone pairs. For all other eclipsed or staggered orientations, a flat potential surface, $V(\Phi_1, \Phi_2)$, for internal rotation with no strongly preferred orientations is expected.

This flat potential leads to rather different structures in the solid and gaseous states (Figure 1 and Table 3). In the crystal, only C_1 symmetric molecules are present. Apparently, this symmetry is favored by packing effects. The dihedral angles of the two molecules in the unit cell adopt values of $\sim 105^\circ$ and $\sim 5^\circ$, that is, both NCO groups nearly eclipse the opposing C–N and C–F bonds, respectively. A different sign for the two dihedral angles implies that both NCO groups lie on the same side of the N1–C3–N2 plane. The two molecules in the unit cell constitute a racemic mixture of two enantiomers. In the gas phase, a mixture of two conformers with C_1 and C_2 symmetry exists in a ratio 72(12)%:28(12)%. This corresponds to $\Delta G^0 = G^0(C_2) - G^0(C_1) = 0.56(18)$ kcal mol $^{-1}$. If we neglect entropy differences between the two conformers and take into account only their different multiplicity (4 for C_1 and 2 for C_2), we obtain $\Delta H^0 = 0.15(18)$ kcal mol $^{-1}$. Thus, within experimental uncertainty, both conformers possess equal enthalpies. This result is reproduced by all quantum chemical calculations that predict energy differences, ΔE , between +0.06 and -0.13 kcal mol $^{-1}$. In the prevailing C_1 symmetric form, the dihedral angles in the gas phase differ by $\sim 25^\circ$ and $\sim 50^\circ$, respectively, from those in the solid phase. One NCO group ($\Phi_1 = 131(4)^\circ$) eclipses one C–F bond and the other group ($\Phi_2 = 43(5)^\circ$) staggers opposite C–N and C–F bonds. In the C_2 form, both groups ($\Phi_1 = \Phi_2 = 52(8)^\circ$) adopt staggered orientations.

The dihedral angles obtained with quantum chemical calculations depend strongly on the computational method (Table 3). According to the HF/6-31G* approximation, one NCO group staggers ($\Phi_1 = 180^\circ$) and the other one eclipses ($\Phi_2 = 0^\circ$) opposite bonds (C_s symmetry), whereas both groups adopt an intermediate orientation with $\Phi_1 = \Phi_2 = 93^\circ$ in the C_2 conformer. MP2 and DFT calculations (B3PW91 and B3LYP) with 6-31G* basis sets result in dihedral angles Φ_1 between 125° and 173° and Φ_2 between 42° and 64° for the C_1 conformer and in $\Phi_1 = \Phi_2$ between 68° and 89° for the C_2 structure. This strong variation of dihedral angles is a consequence of the very flat energy hyperface $V(\Phi_1, \Phi_2)$. This flat hyperface is also demonstrated by two MP2/6-311G(2df) calculations in which the bond lengths and bond angles were optimized and the dihedral angles were fixed at experimental values. The predicted energy for $\Phi_1 = 131^\circ$ and $\Phi_2 = 43^\circ$, which are the gas-phase values for the C_1 conformer, is only 0.16 kcal mol $^{-1}$ higher than that for the optimized values of 173° and 42° , although one NCO group is rotated by $\sim 40^\circ$. Similarly, the X-ray values of 107.2° and -4.7° (molecule A) lead to a small increase in energy of 0.52 kcal mol $^{-1}$. Thus, only weak interactions in the crystal are required to accomplish the rather strong distortion between the gas-phase and solid-state structures. Because of near compensation of anomeric and steric effects, staggered and eclipsed orientations of the NCO groups possess very similar energies in $\text{CF}_2(\text{NCO})_2$. The only other compound that contains two adjacent NCO groups and whose gas-phase structure is known is dichlorosilyl diisocyanate, $\text{Cl}_2\text{Si}(\text{NCO})_2$.¹⁰ The GED intensities are fitted with a C_2 model in which both NCO groups nearly eclipse opposite SiCl bonds ($\Phi(\text{Cl}-\text{Si}-\text{N}=\text{C}) = 14(3)^\circ$). Apparently, the anomeric effect is dominant in this compound and steric repulsions are reduced due to longer bond lengths and a much wider bond angle at nitrogen (136.0 (10°)).

If we consider the systematic differences between geometric parameters obtained by GED and X-ray diffraction due to different vibrational effects and due to interactions in the crystal, the bond lengths and bond angles of solid and gaseous $\text{CF}_2(\text{NCO})_2$ are in excellent agreement (see Table 2). The results obtained with the MP2/6-311G(2df) and B3LYP(6-311G(2df))

methods are also listed in Table 2. All computational methods that include electron correlation effects (MP2 and DFT) reproduce the experimental bond lengths and angles very closely.

Experimental Section

General. A conventional glass vacuum line was used to handle volatile materials. Nuclear magnetic resonance (NMR) spectra were recorded using a JEOL LAMBDA 400 with CFCl_3 (^{19}F), tetramethylsilane (TMS) (^{13}C), and CH_3NO_2 (^{15}N) as reference standards. Infrared (IR) spectra were recorded with a Perkin-Elmer 883 in the gas phase (KBr windows) using a conventional 100 mm gas IR cell. Mass spectra were recorded with a Varian MAT 711 (80 eV). Sodiumdifluoromalonate was provided by DUPONT.

Syntheses. Caution. Acyl azides are explosive. Although we have never observed any explosions during the several times we prepared difluorodiisocyanatomethane by a Curtius Rearrangement, the reaction should be carried out only on a small scale with great care behind a safety shield under a well ventilated hood. We have never attempted to isolate the intermediate acyl azide.

Difluoromalonyl Chloride. A mixture of phosphoryl chloride (35 mL) and disodiumdifluoromalonate was heated slowly to 90°C . After 2 h, all volatile materials were distilled into a trap kept at -196°C under vacuum. The crude product was purified by distillation using a spinning band column (effective length, 40 cm), yielding 12.4 g (65.6%) of difluoromalonyl chloride as a colorless liquid, bp 66°C ; ^{19}F NMR (CDCl_3 , δ): -102.3 ppm; MS m/z (70 eV): 141 [M^+-Cl], 113 [$(\text{CF}_2\text{COCl})^+$], 78 [$(\text{CF}_2\text{CO})^+$], 63 [$(\text{COCl})^+$], 50 [$(\text{CF}_2)^+$].

Difluorodiisocyanatomethane. Difluoromalonyl chloride 4.5 g (33.6 mmol) and 3 mL of toluene were heated to 60°C . Trimethylsilyl azide (7.8 g, 67 mmol) was added over a 45-min period using a syringe, and the reaction temperature was kept at 65°C for an additional hour. On heating to 100°C , a gentle gas evolution could be observed. ^{19}F NMR spectroscopy allowed the monitoring of the reaction. After 16 h, the reaction had come to completeness. Purification by distillation using a spinning band column resulted in a fraction with a bp of 41°C . However, NMR spectroscopy revealed the presence of impurities of fluorotrimethylsilane (5%) and chlorotrimethylsilane (10%). An analytically pure sample was obtained by preparative GLC (squalane/chromosorb, $l = 4$ m, i.d. = 10 mm, $T = 48^\circ\text{C}$) in a yield of 2.1 g (46.6%); ^{19}F NMR (CDCl_3 , δ): -34.9 ppm; ^{13}C (CDCl_3 , δ): 112.6 (t, CF_2 , $^1\text{J}(^{13}\text{C}-^{19}\text{F}) = 250$ Hz), 128.6 (s, NCO) ppm; ^{19}F - ^{15}N HMQC (CDCl_3 , δ): (^{15}N) = -318.0 ($^2\text{J}(^{15}\text{N}-^{19}\text{F}) = 6$ Hz) ppm; IR (gaseous): $\nu = 3686$ (w), 3379 (w), 2513 (w), 2414 (w), 2273 (vs), 1850 (w), 1774 (m), 1449 (s), 1383 (sh), 1132 (s), 1089 (s), 1023 (w), 755 (w), 611 (w), 521 (w) cm^{-1} ; MS m/z (70 eV): 134 [M^+], 115 [$(\text{M}-\text{F})^+$], 108 [$(\text{M}-\text{CN})^+$], 92 [$(\text{M}-\text{NCO})^+$], 64 [$(\text{CF}_2\text{N})^+$], 50 [$(\text{CF}_2)^+$], 42 [$(\text{NCO})^+$].

X-ray Crystal Structure Analysis. Difluorodiisocyanatomethane was condensed into a glass capillary (i.d. 0.3 mm) using a conventional glass vacuum line system by cooling with liquid nitrogen. After a column of 3–4 mm of the liquid was obtained, the capillary was sealed under vacuum at a length of 30 mm. The capillary was mounted on an insulated arcless goniometer head and placed in the stream of cold nitrogen gas of an integrated cooling device²² onto a computer-controlled Siemens four-circle single-crystal diffractometer. Single crystals were grown by setting the temperature of the gas stream to a few degrees below the melting point of the compound of 150 K. The major part of the sample column was molten from its lower

side using a coaxial coil of heating wire. By electronically controlling the heat output of the coil, the phase border face was very slowly moved in the opposite, downward direction. Finally, the crystal was annealed at the preset temperature. After cooling the crystals slowly to 141 K, the X-ray intensity data were collected using MoK radiation with an Nb filter.

The data were corrected by Lorentz-polarization (Lp) and reduced to F_o^2 . The structure solution was obtained by direct methods (SHELXS-97).¹⁴ Full-matrix least-squares refinement based on F^2 (SHELXL-97)¹⁵ with anisotropic displacement parameters converged at $R(F) = 0.043$ for 2721 observed reflections ($F_o^2 > 2(F_\sigma^2)$) and $wR_2 = 0.1179$ for all 4292 crystallographic unique reflections and 163 refined parameters.

Crystal data, experimental conditions, and refinement values are listed in Table 1. The geometric parameters are presented in Tables 2 and 3. Atomic coordinates and thermal parameters (U_{eq}) are listed in Table 4. The molecular structures of $CF_2(NCO)_2$ and the corresponding atomic numbering schemes are depicted in Figures 1 and 2, respectively. A packing diagram is shown in Figure 3.

Gas Electron Diffraction. The GED intensities were recorded with a Gasdiffraktograph KD-G2²³ at 25 and 50 cm nozzle-to-plate distances and with an accelerating voltage of ~60 kV. The sample temperature was -27°C and the inlet system and nozzle were at room temperature. The photographic plates were analyzed with the usual methods,²⁴ and molecular intensities in the s ranges $2-18\text{ \AA}^{-1}$ and $8-35\text{ \AA}^{-1}$, in steps of $\Delta s = 0.2\text{ \AA}^{-1}$, were used in the structure analysis ($s = (4\pi/\lambda)\sin\theta/2$; λ is electron wavelength and θ is scattering angle). Averaged molecular intensities for both nozzle-to-plate distances are shown in the Supporting Information.

Acknowledgment. This work was supported by the Fonds der Chemischen Industrie and the Deutsche Forschungsgemeinschaft (DFG). We are indebted to DUPONT for a sample of disodiumdifluoromalonate.

Supporting Information Available: Tables listing experimental and calculated vibrational amplitudes, details of X-ray data collection and refinement, atomic coordinates and isotropic displacement parameters, bond lengths, angles and dihedral angles of crystal structures and anisotropic displacement parameters. Figure showing experimental and calculated GED intensities for two nozzle-to-plate distances and residuals. This information is available free of charge via the Internet at <http://pubs.acs.org>.

References and Notes

(1) Ulrich, H. In *Ullmann's Encyclopedia of Industrial Chemistry*; Elvers, B., Hawkins, S., Ravencroft, M., Schulz, G., Eds.; VCH: New York 1989; Vol. A14. Chadwick, D. H.; Cleveland, T. H. In *Encyclopedia of Technical Chemistry*; Wiley: New York, 1981. Backus, J. K.; Blue, C. D.; Boyd, P. M.; Cama, F. J.; Chapman, J. H.; Eakin, J. L.; Harasin, S. J.;

McAfee, E. R.; McCarty, C. G.; Nodelman, N. H.; Rieck, J. N.; Schmelzer, H. G.; Squiller, E. P. In *Encyclopedia of Polymer Science and Engineering*; Mark, H. F., Bikales, N. M., Overberger, C. G., Menges, G., Kroschwitz, J. I., Eds.; Wiley: New York, 1988; Vol. 13, p 243. Frisch, K. C.; Klempner, D. In *Comprehensive Polymer Science*; Allen, G., Bevington, J. C., Eastmond, G. C., Ledwith, A., Russo, S., Sigwalt, P., Eds.; Pergamon Press: Oxford, 1989; Vol. 5, p 413.

(2) March, J. *Advanced Organic Chemistry*, 3rd Ed. Wiley: New York, 1985.

(3) Roesch, R.; Gold, M. H. *J. Am. Chem. Soc.* **1951**, *73*, 2959.

(4) Curtius, T.; Gund, R. *J. Prakt. Chem.* **1924**, *107*, 180; Curtius, T.; Gund, R. *J. Prakt. Chem.* **1924**, *107*, 192.

(5) Klöter, G.; Lutz, W.; Seppelt, K.; Sundermeyer, W. *Angew. Chem. Int. Ed. Engl.* **1977**, *16*, 707. Klöter, G.; Seppelt, K. *J. Am. Chem. Soc.* **1979**, *101*, 347.

(6) Barr, D. A.; Haszeldine, R. N. *J. Chem. Soc.* **1956**, 3428. Sprenger, G. H.; Wright, K. J.; Shreeve, J. M. *Inorg. Chem.* **1973**, *12*, 2890. Lidy, W., Sundermeyer, W. *Chem. Ber.* **1976**, *101*, 1491.

(7) Middleton, W. J. *J. Org. Chem.* **1983**, *48*, 3845.

(8) Middleton, W. J., *J. Org. Chem.* **1984**, *49*, 4541.

(9) Rigaudy, J.; Lytwyn, E.; Wallach, P.; Cuong, N. K. *Tetrahedron Lett.* **1980**, *21*, 3367.

(10) Hilderbrandt, R. L.; Bauer, S. H. *J. Mol. Struct.* **1969**, *3*, 325.

(11) Hitchcock, P. B.; Lappert, M. F.; Pierssens, L. J.-M. *Organometallics* **1998**, *17*, 2686.

(12) Frisch, M. J.; Trucks, G. W.; Schlegel, H. B.; Scuseria, G. E.; Robb, M. A.; Cheeseman, J. R.; Zakrzewski, V. G.; Montgomery, J. A.; Stratman, R. E.; Burant, J. C.; Dapprich, S.; Millam, J. M.; Daniels, A. D.; Kudin, K. N.; Strain, M. C.; Farkas, O.; Tomasi, J.; Barone, V.; Cossi, M.; Cammi, R.; Menucci, B.; Pomelli, C.; Adamo, C.; Clifford, S.; Ochterski, J.; Petersson, G. A.; Ayala, P. Y.; Cui, Q.; Morokuma, K.; Malick, D. K.; Rabuck, A. D.; Raghavachari, K.; Foresman, J. B.; Cioslovski, J.; Ortiz, J. V.; Stefanov, B. B.; Liu, G.; Liashenko, A.; Piskorz, P.; Komaromi, I.; Gomperts, R.; Martin, R. L.; Fox, D. J.; Keith, T.; Al-Laham, M. A.; Peng, C. Y.; Nanayakkara, A.; Gonzales, C.; Challacombe, M.; Gill, P. M. W.; Johnson, B.; Chen, W.; Wong, M. W.; Andres, J. L.; Gonzales, C.; Head-Gordon M.; Replogle, E. S.; Pople, J. A. Gaussian, Inc.: GAUSSIAN 98 (Revision A.6); Pittsburgh, PA, 1998.

(13) Hedberg, L.; Mills, I. M. *J. Mol. Spectrosc.* **1993**, *160*, 117.

(14) Sheldrick, G. M. *SHELXS97 - Program for Crystal Structure Solution*; Institut für Anorganische Chemie der Universität: Tammanstrasse 4, D-3400 Göttingen, Germany, 1998.

(15) Sheldrick, G. M. *SHELXL97 - Program for Crystal Structure Analysis (Release 97-2)*; Institut für Anorganische Chemie der Universität, Tammanstrasse 4, D-3400 Göttingen, Germany, 1998.

(16) (a) Spek, A. L. *Acta Crystallogr., Sect A* **1990**, *46*, C34. (b) Spek, A. L. *PLATON, A Multipurpose Crystallographic Tool*; Utrecht University: Utrecht, The Netherlands, 1998.

(17) Sipachev, V. A. *Advances in Molecular Structure Research*, JAI Press: London, 1999; Vol. 5, p 263 ff Sipachev, V. A. *J. Mol. Struct. (THEOCHEM)* **1985**, *121*, 143.

(18) Chang, Y. P.; Su, T. M. *J. Mol. Struct. (THEOCHEM)* **1996**, *365*, 183.

(19) Hamilton, W. *Acta Crystallogr.* **1965**, *18*, 502.

(20) *The Anomeric Effect and Associated Stereoelectronic Effects*; Thatcher, G. R. J., Ed.; ACS Symposium Series No. 539; American Chemical Society: Washington, DC, 1993. Graczyk, P. P.; Mikolajczyk, M. *Top. Stereochem.* **1994**, *21*, 159.

(21) Koput, J.; Stahl, W.; Heineking, N.; Pawelke, W.; Steger, B.; Christen, D. *J. Mol. Spectrosc.* **1994**, *168*, 323.

(22) Dietrich, H.; Dierks, H.; *Messtechnile* (Braunschweig) **1970**, *78*, 184.

(23) Oberhammer, H. *Molecular Structures by Diffraction Methods*, The Chemical Society: London, 1976; Vol 4, p 24.

(24) Oberhammer, H.; Gombler, W.; Willner, H. *J. Mol. Struct.* **1981**, *70*, 273.